ARTICLE

Journal of **Applied Polymer** SCIENCE **WILEY**

PBAT/hybrid nanofillers composites—Part 1: Oxygen and water vapor permeabilities, UV barrier and mechanical properties

Mayara Pollyane Calderaro[1] ● | **Claire Isabel Grígoli de Luca Sarantopóulos**[2] |
Elisabete Maria Saraiva Sanchez[3] | **Ana Rita Morales**[1]

[1]School of Chemical Engineering, University of Campinas, Campinas, Sao Paulo, Brazil

[2]Packaging Technology Center, Institute of Food Technology, Campinas, Sao Paulo, Brazil

[3]Rua Alice Kimaid Farah, Campinas, Sao Paulo, Brazil

Correspondence
Ana Rita Morales, School of Chemical Engineering, University of Campinas, Av. Albert Einstein, 500, 13083-852 Campinas, Sao Paulo, Brazil.
Email: morales@unicamp.br

Abstract

This work evaluated the effect of the combination of nanofillers: organically modified montmorillonite (MMT), sepiolite (SEP) and nano titanium dioxide (TiO$_2$) on the oxygen and water vapor permeability coefficients, light transmission and mechanical properties of poly(butylene adipate-co-terephthalate) (PBAT) aiming at packaging application. The clays concentrations were chosen considering percolation threshold from the clays aspect ratio by TEM analyses. Comparing to neat PBAT, oxygen and vapor permeability coefficients showed reduction with the increase of MMT while SEP and nano-TiO$_2$ did not show significant influence. However, nano-TiO$_2$ was the only filler able to reduce UV and visible light transmission. Nanofillers and their combinations showed to be statistically significant for the increase in Young's modulus, although the tensile strength and elongation showed no influence. The results were discussed in terms of the fillers' morphology and dispersion. Nielsen's model was applied to estimate the aspect ratio of the MMT in nanocomposites.

KEYWORDS

packaging, biodegradable polymer, permeability, nanoclays

1 | INTRODUCTION

The main function of food packaging is to maintain the quality and safety of food products during storage and transport, as well as extending their shelf life in order to act as barriers preventing unfavorable factors or conditions.[1] The increase in the use of plastic materials in flexible packaging for food products leads to concern about the accumulation of plastic waste in landfills generated by the long period of degradation of these materials. Thus, research has been carried out to minimize this environmental problem by replacing conventional polymers with biodegradable ones.[2]

PBAT is a flexible biodegradable copolyester designed for film extrusion.[3] This polymer has great commercial potential mainly due to its easy processing and mechanical properties similar to LDPE[4] and has been considered a promising candidate in the packaging industry, for agricultural films and medicals applications.[1,5,6] As biodegradable polymers commonly present lower mechanical and gas barrier properties when compared with conventional polymers, the use of nanoparticles can improve the mechanical, thermal and barrier properties of these materials.[7–13] The incorporation of nanoparticles, such as silicate, clay, titanium dioxide (TiO$_2$) in biopolymers can provide various functions for food applications, such

as antimicrobial agents, biosensor, oxygen scavenger, and stabilizer to UV radiation.[9]

Nanoclays incorporation is also an important alternative to improve polymers properties. The most commonly used clays in the field of nanocomposites belong to the group of 2:1 layered silicates, also known as 2:1 phyllosilicates, such as montmorillonite and saponite.[14] Layered montmorillonite clay acts as barriers in the polymeric matrix forcing a tortuous pathway for the permeant through the nanocomposite, which is a good feature for permeability reduction.[15] Other promising clay is sepiolite, which is a nonplanar phyllosilicate with fibrous morphology. Sepiolite is a hydrated fibrous magnesium silicate that is included in the 2:1 phyllosilicate group because it contains a continuous two-dimensional tetrahedral sheet of Si_2O_5 composition but differs from the layered silicates because it does not have a continuous octahedral sheet.[16] Sepiolite fiber dimensions can range in length from 0.2 to 4.0 μm, width from 10 to 30 nm and thickness from 5 to 10 nm. Its blocks are not sheets, but ribbons that are attached and form an open channel that resembles that of zeolites. Sepiolite presents high surface area (BET $374 \pm$ m²/g), which is expected to provide the material with good water vapor and oxygen barrier property in addition to improvements in mechanical properties.[2,5,16] To date, no reports have been found on the performance of this clay in the PBAT matrix to improve barrier property.

Another important factor for packaging is protection against photodegradation. Photodegradation can affect both the packaging with polymer degradation and the product to be packaged with photo-oxidation process, causing food to have reduced shelf life, color loss, and undesirable odors and flavors. For the ultraviolet radiation protection, titanium dioxide (TiO_2) has been reported to prevent UV transmission even at very low concentration[17,18] showing highest UV blocking power for the rutile and nanosized TiO_2,[19] which justified a nano-TiO_2 ($nTiO_2$) to be the system under study.

The different morphology of the nanofillers as lamellar, needles and spherical particles showed to provide interaction between them and the formation of some different arrangements resulting in specific properties for PBAT as discussed in this work in terms of morphology and fillers level of dispersion supported by statistical analysis. The aspect ratio of the MMT on nanocomposites was estimate by Nielsen's model to estimated its dispersion level.

2 | MATERIALS AND METHODS

2.1 | Materials

PBAT Ecoflex® F blend C1200 from BASF Chemical Company (density: 1.27 g/cm³); nanoclay montmorillonite Closite 30B (MMT) from Southern Clay (density: 1.859 g/cm³); and Sepiolite 70253 (SEP) supplied by Sigma Aldrich (density: 2.329 g/cm³). DuPont Light Stabilizer 210 nano titanium dioxide ($nTiO_2$) was supplied by DuPont.

2.2 | Determination of clays concentrations

First, MMT concentrations to provide the material with the target value of 5,000 cm³ μm m⁻² d⁻¹ atm⁻¹ for O_2 permeability coefficient was calculated using the Nielsen's model,[15] according to Equation (1).

$$\frac{P_{\text{nano}}}{P_{\text{matrix}}} = \frac{1 - \phi}{1 + \frac{\alpha.\phi}{2}} \qquad (1)$$

where P_{nano} is the nanocomposite permeability coefficient, assuming 5,000 cm³μm m⁻² d⁻¹ atm⁻¹ as the goal of this study (equivalent to oxygen transmission rate of 100 cm³m⁻²d⁻¹ considering a film with thickness of 50 μm at 23°C); P_{matrix} is the matrix permeability coefficient, 60,000 cm³ μm m⁻² d⁻¹ atm⁻¹ (equivalent to oxygen transmission rate of 1,200 cm³m⁻²d⁻¹ considering a film with thickness of 50 μm based on supplier data[20]; ϕ is the volume fraction of the nanoplatelets that are dispersed in the matrix; and α is the aspect ratio of nanoplatelets (α = L/D, L= length and D= thickness); for montmorillonite L/D = 600 obtained by transmission electron microscopy (TEM) (Figure 1).

Sepiolite concentrations were based on the percolation threshold theory, defined as the volumetric fraction of nanoclay required to form a continuous network capable of favoring the distribution of stresses in the composite,[21,22] according to Equation (2).

$$\phi_v = \frac{0.7}{\frac{L}{D}} \qquad (2)$$

where ϕ_v = volume fraction of the percolation threshold; L/D is the aspect ratio of nanoclay (sepiolite L/D = 32 obtained by transmission electron microscopy (TEM) (Figure 1).

We calculated mass concentrations based on the calculated volume fraction of the nanoclays and density of the materials. Therefore, the mass concentration for MTT to achieve the permeability target was calculated as 7%, considering 30% of organic salt, and for SEP, the mass concentration at the percolation threshold was 4%. These numbers were the base for the design of experiments.

FIGURE 1 Micrographs obtained by TEM for (a) montmorillonite, (b) sepiolite clay and (c) nano titanium dioxide
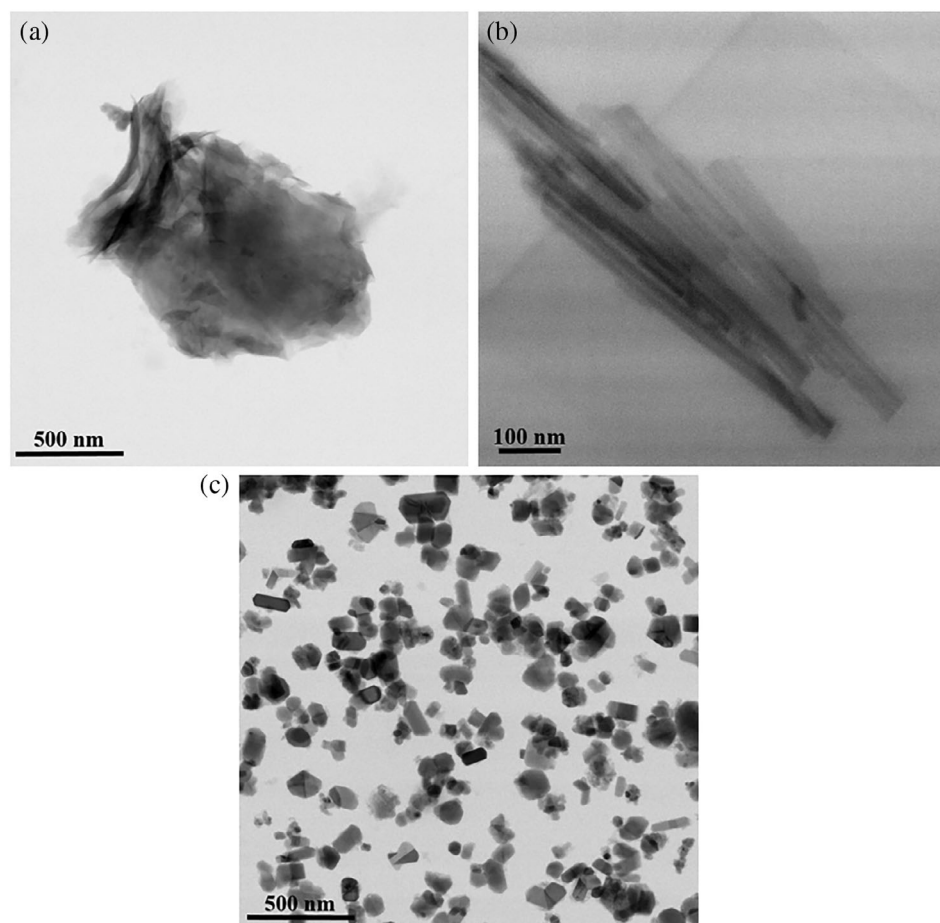
2.3 | Design of experiments

In order to verify the influence of nanofillers incorporated in the matrix and their interactions a 2^3 factorial rotatable central composite design ($\alpha = 1.682$) with three central points was conducted. The experimental matrix is presented in Table 1. There are five different concentrations in percent by mass for each compound. Concentrations of percolation for nanoclays were used at levels +1 so that the formulations did not exceed the total of 15% of fillers. $nTiO_2$ was added as 1 part of additive per hundred parts of resin (1 phr). The data were analyzed using STATISTIC 7.0 software (Statsoft, USA) with analysis of variance (ANOVA) at 95% of confidence level and pure error.

Reference formulations have been produced for comparison with samples of the design of experiments. Reference samples are not part of the DoE and have concentrations at the central point of each nanofiller concentration. By analyzing these samples the influence of isolated nanofiller in the polymer could be known. Reference samples are: PBAT (neat PBAT), PBAT+MMT4.5 (PBAT with 4.5% in mass of MMT), PBAT+SEP2.5 (PBAT with 2.5% in mass of SEP), and PBAT+$nTiO_2$0.7 (PBAT with 0.7% in mass of $nTiO_2$).

2.4 | Preparation of nanocomposites

Prior to the mixing step, PBAT was dried at 70°C for 1 hr, and the clays were dried at 70°C for 5 hr. The components of each formulation were mixed in a DRAIS homogenizer (M.H. Equipments, MH-100) and the samples were prepared by hot-pressing at 150°C and pelletized in a granulator. The films were prepared in a blowing extruder (AX Plásticos, AX16/26) L/D=26 with speed of approximately 7 rpm. The processing was carried out with the following temperature profile: Zone 1=130°C; Zone 2=140°C, and Zone 3=150°C. The films with thickness of 50 to 55 μm were used for characterization.

2.5 | Transmission electron microscopy

TEM analysis was performed to evaluate the nanofillers morphology using a FEI TECNAI G^2 F20 HRTEM 200 kV microscope. The samples were dispersed in isopropyl alcohol and then deposited with copper-coated copper grids. The aspect ratio (L/D) of the nanoparticles was determined from the diameter (D) and length

TABLE 1 2^3 rotatable central composite design ($\alpha = 1.682$) with three central points

Assay	Coded level			Actual concentration (% by mass)			Samples
	X1	X2	X3	MMT	SEP	nTiO$_2$	
1	–	–	–	2	1	0.2	M2S1T0.2
2	–	–	+	2	1	1.2	M2S1T1.2
3	–	+	–	2	4	0.2	M2S4T0.2
4	–	+	+	2	4	1.2	M2S4T1.2
5	+	–	–	7	1	0.2	M7S1T0.2
6	+	–	+	7	1	1.2	M7S1T1.2
7	+	+	–	7	4	0.2	M7S4T0.2
8	+	+	+	7	4	1.2	M7S4T1.2
9	−1.682	0	0	0	2.5	0.7	M0S2.5 T0.7
10	1.682	0	0	9	2.5	0.7	M9S2.5T0.7
11	0	−1.682	0	4.5	0	0.7	M4.5S0T0.7
12	0	1.682	0	4.5	5	0.7	M4.5S5T0.7
13	0	0	−1.682	4.5	2.5	0	M4.5S2.5T0
14	0	0	1.682	4.5	2.5	1.5	M4.5S2.5T1.5
15	0	0	0	4.5	2.5	0.7	M4.5S2.5T0.7
16	0	0	0	4.5	2.5	0.7	M4.5S2.5T0.7
17	0	0	0	4.5	2.5	0.7	M4.5S2.5T0.7

Note: Matrix coded, decoded (nanoparticles concentration), and nomenclature of the nanocomposites samples.

(L) from TEM images using the ImageJ software. Approximately 30 measurements were taken for each nanoclay and 150 measurements for calculating the average particle diameter of nTiO$_2$.

2.6 | Light transmission

Light transmission (%T) of the films was measured using a UV–visible spectrophotometer (SPECORD 210, Analytic Jena) with integrated sphere, $\Delta\lambda$ of 2 nm and speed of 2 nm/s. For each formulation three specimens with a mean thickness of 50 μm were scanned using 300–800 nm wavelength. Mean light transmission percentage was calculated from the integrated area under the light transmission spectrum divided by the bandwidth, from 100 nm to UV radiation and 400 nm to visible light. The %T was taken as the ability of the filler to block UV and visible light.

2.7 | Oxygen permeability

Oxygen transmission rate (OTR) of films was measured using an Oxygen Permeation Analyzer (OX-TRAN® 2/20, Mocon) with coulometric sensor, according to the ASTM

D 3985-05, at 23°C and dry conditions. The analyses were performed in duplicate. The oxygen permeability coefficient (OP) was calculated using Equation 3.

$$OP = OTR\left(\frac{l}{p_1 - p_2}\right) \tag{3}$$

where OP is the oxygen permeability coefficient (cm^3 μm m^{-2} d^{-1} atm^{-1}), OTR is the oxygen transmission rate (cm^3 m^{-2} d^{-1}), l is the film thickness (μm), p_1 is the pressure of the gas at the test temperature on the film test side and p_2 is the partial pressure on the detector side (equal to zero).

2.8 | Water vapor permeability

Water vapor transmission rate (WVTR) of films was estimated by the desiccant method at 38°C and 90% relative humidity according to ASTM E-96-95. The specimens were conditioned at 50% RH at 25°C for 24 hr, after being placed in partially filled test dishes with CaCl$_2$ ($\sim$30 g). The analyses were performed in duplicate and a blank (test dish without the addition of CaCl$_2$) was used for each sample. The films were adhered in adhesive aluminum masks with a circular permeation area of 5 cm^2, which were fixed in the test dishes. Periodic weighing

was performed at each hour. Water vapor permeability coefficient (WVPC) were expressed in g μm m^{-2} d^{-1} mmHg^{-1}, according to Equation 4.

$$WVPC = \frac{WVTR.l}{P_S \left(\frac{RH_1 - RH_2}{100} \right)} \quad (4)$$

where WVPC is the water vapor permeability coefficient (g μm m^{-2} d^{-1} mmHg^{-1}), WVTR is the water vapor transmission rate (g m^{-2} d^{-1}), l is the film thickness (μm), P_s is the saturation vapor pressure at test temperature (49.692 mmHg at 38°C), RH_1 is the relative humidity in the test chamber, and RH_2 is the relative humidity inside the test dish.

2.9 | Mechanical properties

Tensile strength tests were performed according to ASTM D882-12 with nine specimens for each formulation. The samples were preconditioned at 23°C for 48 hr and 50% relative humidity. The tests were carried out on uniaxial tensile equipment (Tinius Olsen, H5KS) with speed of 500 mm/min, a load cell of 5000 N at 23°C.

3 | RESULTS AND DISCUSSIONS

3.1 | Transmission electron microscopy

The morphology of the nanoclays and nano titanium dioxide was analyzed as shown in Figure 1. MMT showed a lamellar structure and irregular profile with mean length (L) of 600 nm. Considering that nanoplatelets of the layered silicate clays have thickness (D) of approximately 1 nm,[23] the aspect ratio (α = L/D) for the MMT was estimated as 600. Natural sepiolite has a fibrous morphology composed of long structures similar to needles arranged in parallel[24] with an average L of 550 nm and D of 17 nm that result in L/D of 32. These fibers form agglomerates due to the surface interaction between the individual particles, similar behavior was observed by Liang et al.[25] The particles shape of nTiO$_2$ is shown in Figure 1c with average particle size of 132 nm.

3.2 | Light transmission

The light transmission percentage (% T) values of all samples are presented in Table 2, and the curves for the reference samples are presented in Figure 2, where we observe that only the PBAT+nTiO$_2$ 0.7 had a decrease in light transmission percentage when compared with neat PBAT, from 50.3% to 11.9% in the UV radiation regions and from 75.7% to 60.0% in the visible region radiation. Based on Figure 2 and Pareto's chart in Figure 3, we conclude that only nTiO$_2$ was statistically significant and that the higher the nTiO$_2$ concentration the lower the transmittance, showing that nanoclays concentration did not play any important role in the %T in UV and visible region with 95% confidence. This result was expected since metal oxide, as titanium dioxide, has a good ultraviolet blocking power.[19] Besides, this behavior could be attributed to the refractive index of particles. Titanium dioxide has a refractive index around 2.62 for rutile and 2.55 anatase,[26] while clay minerals, in general, have a refractive index within range from 1.47 to 1.68,[27,28] close to refractive index of the polyesters 1.52 to 1.57.[28,29] Thus, both MMT and SEP have very similar light scattering power as polyesters and do not act as UV and light filters.[28]

The ANOVA for UV radiation is shown in Table 3. The model is considered statistically significant because the calculated F = 129.29 (regression/residual) is much larger than the critical F = 3.68 value at 95% confidence. The model also shows no lack of fit, since the calculated F = 2.45 (lack of fit/pure error) is less than the value of tabulated F = 19.30, thus assuming that the model is predictive.

The ANOVA for visible light region is show in Table 4. The model is considered statistically significant and predictive, since the calculated F (regression/residual) is higher than the critical F value at 95% confidence and the calculated F (lack of fit/pure error) is less than the value of tabulated F.
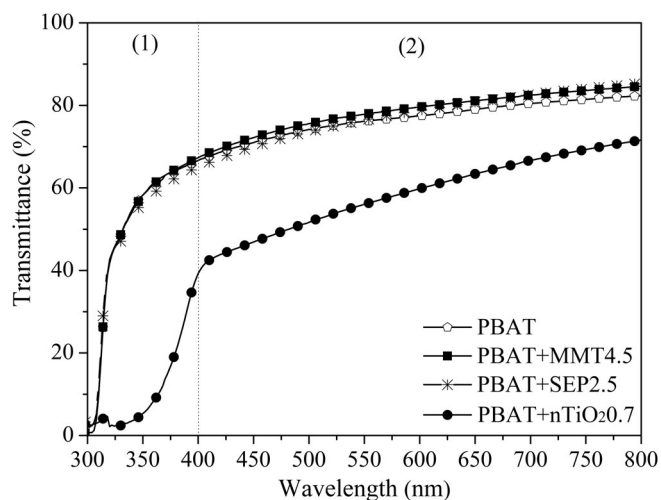

FIGURE 2 UV–Vis spectra of neat PBAT and nanocomposites

TABLE 2 General properties of PBAT and nanocomposites

Sample	UV/Vis transmission		Oxygen permeability		Water vapor permeability		Mechanical properties		
	UV (300–400 nm) (%)	Visible (400–800 nm) (%)	OP^a ($cm^3 \, \mu m \, m^{-2} \, day^{-1} \, atm^{-1}$)	Reduction (%)	WVP^b ($g \, \mu m \, m^{-2} \, d^{-1} \, mmHg^{-1}$)	Reduction (%)	Stress at break (MPa)	Elongation (%)	Young's modulus (MPa)
M2S1T0.2	25.3 ±0.1	66.2 ± 1.3	43,262 ±1,571	32	322 ± 25.5	26	19 ± 2	585 ± 34	90 ± 12
M2S1T1.2	5.5 ± 0.7	47.9 ± 3.1	54,181 ±7,020	14	392 ± 12.2	11	20 ± 4	590 ± 91	85 ± 11
M2S4T0.2	24.3 ± 1.8	64.6 ± 1.3	58,471 ±3,473	8	449 ± 22.2	−3	25 ± 4	612 ± 59	97 ± 12
M2S4T1.2	6.0 ± 0.8	51.7 ± 2.2	44,220 ±1,383	30	380 ± 37.3	13	22 ± 2	598 ± 55	114 ± 8
M7S1T0.2	25.9 ± 0.6	69.1 ± 1.2	43,805 ±6,183	31	264 ± 10.4	40	23 ± 4	631 ± 75	107 ± 7
M7S1T1.2	6.0 ± 0.2	52.4 ± 1.4	34,989 ± 40	45	259 ± 1.5	41	20 ± 2	626 ± 53	121 ±14
M7S4T0.2	27.1 ± 1.4	69.4 ± 1.7	35,554 ± 90	44	298 ± 1.1	32	18 ± 2	573 ± 57	125 ± 9
M7S4T1.2	5.3 ± 0.9	50.6 ± 4.1	33,720 ±2,442	47	238 ± 8.0	46	21 ± 2	581 ± 37	153 ±12
M0S2.5T0.7	12.2 ± 0.9	59.3 ± 3.7	59,295 ±2,458	6	389 ± 6.6	11	20 ± 4	555 ± 83	82 ± 3
M9S2.5T0.7	10.3 ± 0.8	57.9 ± 2.8	33,420 ±4,317	47	223 ± 6.5	49	19 ± 3	600 ± 67	130 ± 11
M4.5S0T0.7	10.6 ± 0.8	56.8 ± 1.6	45,516 ±6,597	28	264 ± 8.5	40	22 ± 3	612 ± 51	99 ± 7
M4.5S5T0.7	9.7 ± 0.1	56.1 ± 0.5	41,248 ±4,334	35	280 ± 7.9	36	24 ± 6	680 ± 72	123 ± 7
M4.5S2.5T0	41.7 ± 1.4	68.8 ± 0.9	53,401 ±4,106	16	334 ± 9.0	24	19 ± 2	541 ± 60	108 ± 14
M4.5S2.5T1.5	4.7 ± 0.4	47.8 ± 0.7	42,142 ±5,116	33	301 ± 15.0	31	24 ± 5	694 ± 65	119 ± 10
M4.5S2.5T0.7	10.8 ± 0.5	55.7 ± 1.0	38,350 ±4,711	39	272 ± 7.9	38	21 ± 3	638 ± 61	118 ± 12
M4.5S2.5T0.7	10.2 ± 0.3	59.9 ± 1.1	41,213 ±7,505	35	305 ±0.9	30	22 ± 3	656 ± 38	118 ± 12
M4.5S2.5T0.42	9.1 ± 0.5	58.6 ± 1.1	42,847 ±6,146	32	303 ± 0.9	31	21 ± 5	603 ± 78	89 ± 19
PBAT	50.3 ± 1.4	75.7 ± 1.0	63,214 ±1,879	0	438 ± 3.4	0	21 ± 2	631 ± 64	48 ± 5
PBAT +MMT4.5	49.9 ± 2.5	77.9 ± 3.0	49,931 ±3,222	21	331 ± 11.5	24	27 ± 6	719 ± 43	67 ± 4
PBAT+SEP2.5	49.5 ± 1.0	76.8 ± 1.3	62,541 ± 663	1	437 ± 7.3	0	22 ± 3	572 ± 61	53 ± 4
PBAT +nTiO₂0.7	11.9 ± 1.0	60.0 ± 1.2	50,783 ± 777	20	410 ± 16.8	6	22 ± 4	600 ± 58	52 ± 8

^{a}23°C at dry condition and O_2 partial pressure gradient (1 atm).
^{b}Relative humidity of 90% and temperature of 38°C.

3.3 | Oxygen permeability

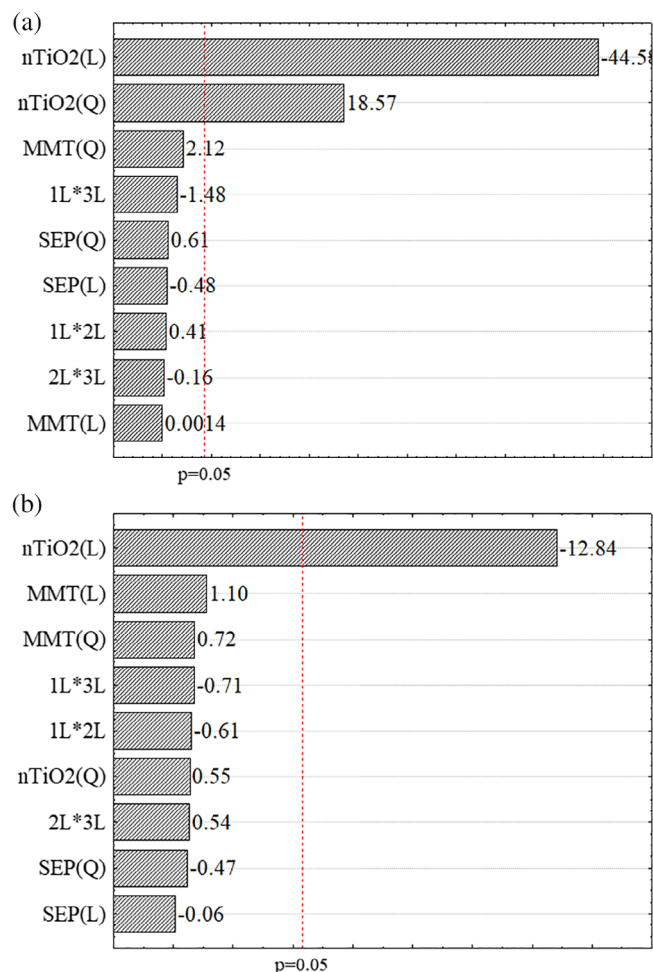Table 2 shows the results for oxygen permeability coefficients (OP) and the reduction (%) in relation to neat

FIGURE 3 Pareto's chart: (a) UV radiation and (b) visible region [Color figure can be viewed at wileyonlinelibrary.com]

PBAT. Based on the statistical analysis, presented in Pareto's chart (Figure 4a), only MMT presented statistically significant results at 95% confidence. The higher the MMT addition to the polymer matrix, the lower the OP of the film. All nanocomposites with MMT presented lower OP values compared with neat PBAT. This phenomenon can be attributed to an intercalated and/or exfoliated structure of MMT in nanocomposites and, consequently, the formation of a tortuous path for oxygen permeation.[11] In general, the reduction of the permeability of a nanocomposite with the incorporation of clays with lamellar structures, is mainly related to the exfoliation of the clay in the polymer matrix, forming a tortuous diffusion path for gases. This exfoliation is dependent on the chemical structure of the clay, its organic modification, as well as the concentration and method of preparation of the nanocomposite.[30] Sepiolite clay has high surface area and it was promising to form a tortuous path for the permeation of gases and water vapor; however, the results were inconsistent with this hypothesis. Probably, the concentration of this clay did not reach percolation and/or agglomerates may have been formed, which may have been caused by its needle-shaped morphology. Moreover, poor or lack of adhesion in the polymer/clay interface could lead to the formation of micro voids that allow greater permeation.[30]

According to the ANOVA (Table 5), the model is considered statistically significant and predictive, since the calculated F (regression/residual) is higher than the critical F value at 95% confidence and the calculated F (lack of fit/pure error) is less than the value of tabulated F.

3.4 | Water vapor permeability

Table 2 shows the values obtained for water vapor permeability coefficients (WVP) and loss percentage of WVP

TABLE 3 Analysis of variance (ANOVA) for %T on UV region

Source of variation	Sum of squares	Degrees of freedom	Mean squares	F test
Regression	1,759.17	9	195.46	129.29[a]
Residue	10.58	7	1.51	
Lack of fit	9.10	5	1.82	2.45[b]
Pure error	1.49	2	0.74	
Total	1,769.75	16		
% explained variation (R^2)	99.40			
% max explained variation	99.92			

Note: F(table)9.7 = 3.68 at 95% level of confidence for the regression (regression/residue).[c] F(table)5.2 = 19.30 at 95% level of confidence for the regression (lack of fit/pure error).[c]
[a]F Test calculated to verify the model statistical significance.
[b]F Test calculated to verify the model lack of fit.
[c]Values calculated by STATISTICA 7.0 software.

TABLE 4 Analysis of variance (ANOVA) for % T on visible light region

	Sum of squares	Degrees of freedom	Mean squares	
Regression	779.12	9	86.57	12.99[a]
Residue	46.64	7	6.66	
Lack of fit	37.39	5	7.48	1.62[b]
Pure error	9.25	2	4.62	
Total	825.76	16		
% explained variation (R^2)	94.35			
% max explained variation	98.88			

Note: F(table)9.7 = 3.68 at 95% level of confidence for the regression (regression/residue).[c] F(table)5.2 = 19.30 at 95% level of confidence for the regression (lack of fit/pure error).[c]
[a]F Test calculated to verify the model statistical significance.
[b]F Test calculated to verify the model lack of fit.
[c]Values calculated by STATISTICA 7.0 software.
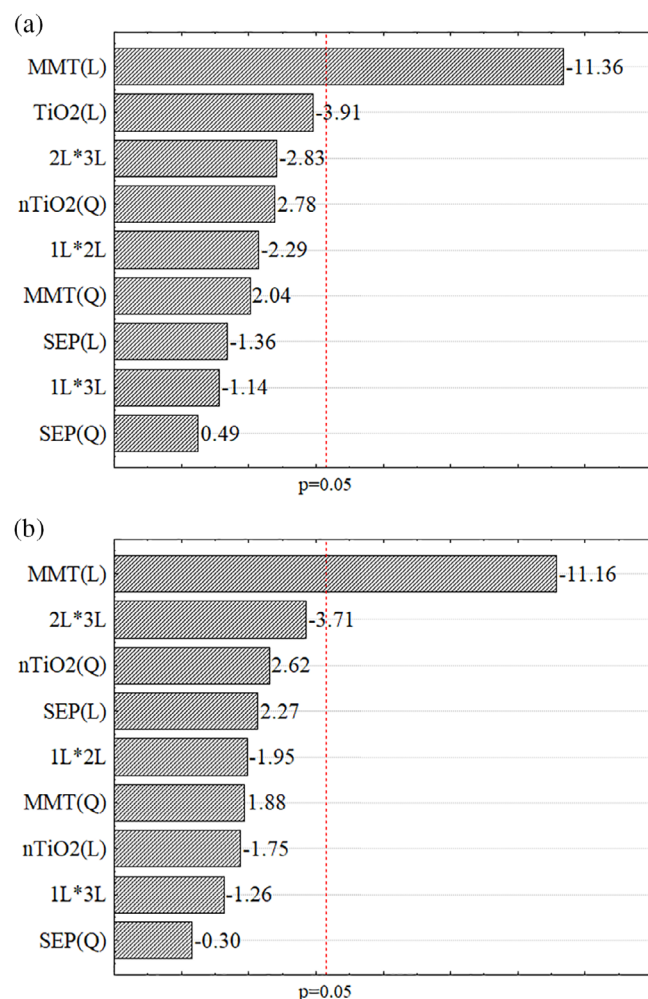
FIGURE 4 Pareto's chart: (a) O_2 permeability coefficient and (b) water vapor permeability coefficient [Color figure can be viewed at wileyonlinelibrary.com]

samples in relation to neat PBAT, and Pareto's chart is shown in Figure 4b. Similarly to OP only MMT was the statistically significant factor, contributing to the decrease of WVP in the samples, and the others fillers did not influence this property. The M7S1T1.2, M7S4T1.2, and M9S2.5T0.7 samples presented better results for water vapor barrier and these results are consistent with the behavior observed by O_2 permeability coefficient analysis. The observed reduction of up to 47% in OP and 49% in WVP is relevant considering food packaging and other applications requiring efficient polymeric barriers. As previously discussed in O_2 permeability coefficient analysis, these results reinforce the hypothesis that this effect could be associated with good delamination and dispersion of MMT in the polymeric matrix, i.e., high exfoliation degree, which forces water vapor to cross a path tortuous, extending the length of the path through which water molecules pass.[11]

According to the ANOVA for WVP (Table 6), the model is considered statistically significant and predictive, since the calculated F (regression/residual) is higher than the critical F value at 95% confidence and the calculated F (lack of fit/pure error) is less than the value of tabulated F.

3.5 | Application of the Nielsen's model to oxygen and water vapor permeability coefficients

Clay apparent aspect ratio can be estimated using the Nielsen's model (Equation 1). Therefore, based on the results obtained from the permeability coefficients, indirectly, MMT dispersion can also be estimated. The Nielsen's model, for the permeability of gases in

TABLE 5 Analysis of variance (ANOVA) for O_2 permeability coefficient

Source of variation	Sum of squares	Degrees of freedom	Mean squares	F test
Regression	883,840,566.41	9	98,204,507.4	3.90[a]
Residue	176,330,678.06	7	25,190,096.9	
Lack of fit	165,967,433.4	5	33,193,486.7	6.41[b]
Pure error	10,363,244.7	2	5,181,622.3	
Total	1,060,171,244.5	16		
% explained variation (R^2)	83.37			
% max explained variation	99.02			

Note: F(table)9.7 = 3.68 at 95% level of confidence for the regression (regression/residue).[c] F(table)5.2 = 19.30 at 95% level of confidence for the regression (lack of fit/pure error).[c]
[a]F Test calculated to verify the model statistical significance.
[b]F Test calculated to verify the model lack of fit.
[c]Values calculated by STATISTICA 7.0 software.

TABLE 6 Analysis of variance (ANOVA) for water vapor permeability coefficient

Source of variation	Sum of squares	Degrees of freedom	Mean squares	F test
Regression	55498.53	9	6166.50	9.31[a]
Residue	4635.94	7	662.28	
Lack of fit	3951.28	5	790.26	2.31[b]
Pure error	684.67	2	342.33	
Total	60134.47	16		
% explained variation (R^2)	92.29			
% max explained variation	98.86			

Note: F(table)9.7 = 3.68 at 95% level of confidence for the regression (regression/residue).[c] F(table)5.2 = 19.30 at 95% level of confidence for the regression (lack of fit/pure error).[c] F(table)5.2 = 19.30 at 95% level of confidence for the regression (lack of fit/pure error).[c]
[a]F Test calculated to verify the model statistical significance.
[b]F Test calculated to verify the model lack of fit.
[c]Values calculated by STATISTICA 7.0 software.

TABLE 7 Aspect ratio (α) from the Nielsen's model for OP and WPV

			OP		WPV	
Samples	% MMT	φ	P_{nano}/P_{matrix}	αOP	P_{nano}/P_{matrix}	αWPV
MMT4.5	4.5	0.022	0.79	22	0.76	27
M7S1T1.2	7.0	0.034	0.55	44	0.59	37
M7S4T1.2	7.0	0.034	0.53	47	0.54	45
M9S2.5 T0.7	9.0	0.044	0.53	36	0.51	40

nanocomposites, assumes that the inorganic nanofiller is completely exfoliated, rectangular with width L and thickness D, perpendicular oriented to the diffusion direction, and the crystallinity percentage remains unchanged with the addition of the fillers.[31] The Nielsen's model was used for the nanocomposites that presented greater reduction in OP and WVP as shown in Table 7.

The aspect ratio (α) found by the application of the Nielsen's model is a strong indicative of the degree of delamination of the clay since the more exfoliated and/or the smaller the number of agglomerates the larger the α value. Considering that a clay nanolayer has a thickness of approximately 1 nm,[23] α corresponds to the mean length in nm of the impermeable specimens. The M7S4T1.2 sample presented the highest α with values of

45–47, being the one with the best exfoliation. The formulation of this sample is the one proposed to achieve the O_2 permeability target according to the Nielsen's model (MMT) and percolation threshold concentration (SEP). As α for MMT was estimated as 600, we can conclude that the clay kept some fraction of tactoids. By comparing the PBAT + MMT4.5 sample that only has the clay MMT in its composition and the smallest aspect ratio[22–27] with the others samples, we can observe that sepiolite and TiO_2 acted so as to improve MMT exfoliation.

3.6 | Mechanical properties

Table 2 reports the mechanical properties: Young's modulus, stress at break, and elongation of neat PBAT and its nanocomposites. No significant variations were observed for stress at break and elongation. Pareto's charts are not

FIGURE 5 Pareto's chart for Young's modulus [Color figure can be viewed at wileyonlinelibrary.com]

shown. On the other hand, all the linear and quadratic factors and the factors interactions were statistically significant for Young's modulus, as reported in Figure 5. The MTT factor (linear) was the most significant and its effect was positive, that is, the greater the MTT concentration the higher the Young's modulus. As shown in Table 2, this property increased about 3 times, from 48.1 MPa to 153 MPa, when comparing neat PBAT with the M7S4T1.2 formulation, respectively. The sample M7S4T1.2 present the most significant reduction in permeability to oxygen and water vapor, it is worth emphasized that this sample has the MMT concentration estimated to the target in O_2 permeability (according to the Nielsen's model) and SEP concentration is the calculated to achieve the percolation threshold.

The increase in Young's modulus could be attributed to a good dispersion of nanoclays, as well as a good interaction between the nanoclays indicating a synergistic effect. The samples containing two or more fillers presented higher modulus results than the isolated fillers. The reference samples did not show changes in stress and elongation, as well as the formulations from the experiment design. Only the sample with incorporation of 4.5% MMT presented greater increase in Young's modulus in relation to the neat PBAT. Sepiolite has a surface area of approximately 300 m^2/g, and a high density on its surface due to silanol groups (-SiOH), which make this clay promising candidate for improving mechanical and barrier properties.[32] It was expected that SEP alone in the PBAT would show significant results in the evaluated properties, but sample with only SEP did not influence tensile properties. This behavior is probably induced by the lower affinity between clay/polymer, since SEP has no surface treatment.[33]

The ANOVA for Young's modulus is shown in Table 8. The calculated F value (regression/residual) is higher than

TABLE 8 Analysis of variance (ANOVA) for Young's modulus

Source of variation	Sum of squares	Degrees of freedom	Mean squares	F test
Regression	5,050.04	9	6,166.50	35.55[a]
Residue	110.48	7	662.28	
Lack of fit	108.54	5	790.26	22.30[b]
Pure error	1.95	2	342.33	
Total	5,160.52	16		
% explained variation (R^2)	97.86			
% max explained variation	99.96			

Note: F(table)9.7 = 3.68 at 95% level of confidence for the regression (regression/residue).[c] F(table)5.2 = 19.30 at 95% level of confidence for the regression (lack of fit/pure error).[c]
[a]F Test calculated to verify the model statistical significance.
[b]F Test calculated to verify the model lack of fit.
[c]Values calculated by STATISTICA 7.0 software.

the critical value at 95% confidence, indicating that the regression is statistically significant. On the other hand, the model does not fit the experimental data well, since the calculated F value (lack of fit/pure error) is higher than the critical value at 95% confidence (i.e., at this confidence level, there is evidence of lack of fit for the model).

4 | CONCLUSIONS

It was found that the clays used do not provide the material with ultraviolet radiation protection. On the other hand, nano-TiO_2 presented a barrier in both the ultraviolet and visible light wavelengths, emphasizing that the protection against visible radiation is very important for packaging application.

For both oxygen and water vapor permeability coefficients only montmorillonite clay showed to be statistically significant to reduce PBAT permeability, although the presence of the others fillers might help the montmorillonite exfoliation so that the barrier properties were even better. The combination of the fillers effect was more pronounced on the mechanical properties, mainly for Young's modulus up to 3 times higher compared with the pure polymer.

The Nielsen's model was applied to achieve an O_2 permeability coefficient target of 5,000 $cm^3.\mu m.m^{-2}.d^{-1}.atm^{-1}$ and the best result obtained was about 33,000 $cm^3.\mu m.m^{-2}.day^{-1}.atm^{-1}$. The expected value was not reached probably because montmorillonite was intercalated and partially exfoliated and in disorientated configuration in nanocomposites, since the Nielsen's model assumes that the clay lamellae are completely exfoliated and oriented perpendicular to the direction of the diffusion flow of permeant. However, although the defined permeability target has not been reached, it is important to note that the combination of the different nanofillers attributed to PBAT a significant reduction of 47% in oxygen permeability and 49% in water vapor permeability. For being an unprecedented study it motivates the continuity of researches with the use of these fillers.

In this study, some hypotheses were raised about the behavior of these nanofillers in the system, exfoliation of MMT and dispersion of nanoparticles in PBAT matrix. The complementary discussion related to these aspects based on rheological, morphological, and XRD analyses will be presented in continuation of this study.

ORCID

Mayara Pollyane Calderaro [ID] https://orcid.org/0000-0001-7025-9075

REFERENCES

[1] J. W. Rhim, H. M. Park, C. S. Ha, *Prog. Polym. Sci.* **2013**, *38*, 1629.

[2] Olivato, J. B.; Marini, J.; Pollet, E; Yamashita, F.; Grossmann, M.V.E.; Avérous, L. *Carbohyd. Polym.* **2015**. *118*, 250.

[3] R. Al-Itry, K. Lamnawar, A. Maazouza, *Polym. Degrad. Stabil.* **2012**, *97*, 1898.

[4] T. Kijchavengkul, R. Axuras, M. Rubino, S. Selke, M. Ngouajio, R. T. Fernandez, *Polym. Degrad. Stabil.* **2010**, *95*, 2641.

[5] K. Fukushima, M.-H. Wu, S. Bocchini, A. Rasyida, M.-C. Yang, *Mater. Sci. Eng. C* **2012**, *32*, 1331.

[6] D. Wei, H. Wang, H. Xiao, A. Zheng, Y. Yang, *Carbohyd. Polym.* **2015**, *123*, 275.

[7] A. Javadi, Y. Srithep, J. Lee, S. Pilla, C. Clemons, S. Gong, L.-S. Turng, *Compos. Part A Appl. Sci. Manuf.* **2010**, *41*, 982.

[8] J.-J. Chen, C.-C. Chen, M.-C. Yang, *J. Polym. Res.* **2011**, *18*, 2151.

[9] S. H. Othman, *Agric. Agric. Sci. Proc.* **2014**, *2*, 296.

[10] J.-H. Chen, M.-C. Yang, *Mater. Sci. Eng. C.* **2015**, *46*, 301.

[11] J. Xie, K. Zhang, J. Wu, G. Ren, H. Chen, J. Xu, *Appl. Clay Sci.* **2016**, *126*, 72.

[12] S. Adrar, A. Habi, A. Ajji, Y. Grohens, *Appl. Clay Sci.* **2017**, *146*, 306.

[13] P.-G. Ren, X.-H. Liu, *Polym. Test.* **2017**, *58*, 173.

[14] P. Bordes, E. Pollet, L. Avérous, *Prog. Polym. Sci.* **2009**, *34*, 125.

[15] G. Choudalakis, A. D. Gotsis, *Eur. Polym. J.* **2009**, *45*, 967.

[16] E. Bilotti, R. Zhang, H. Deng, F. Quero, H. R. Fischer, T. Peijs, *Compos. Sci. Technol.* **2009**, *69*, 2587.

[17] A. Vejdan, S. M. Ojagh, A. Adeli, M. Abdollahi, *Food. Sci. Technol. (Campinas)* **2016**, *71*, 88.

[18] Y. Li, Y. Jiang, F. Liu, F. Ren, G. Zhao, X. Leng, *Food Hydrocoll.* **2011**, *25*, 1098.

[19] H. Yang, S. Zhu, N. J. Pan, *Appl.Polym. Sci.* **2004**, *92*, 3201.

[20] BASF Ecoflex® F Blend C1200. Product Information and Brochure, **2013**. https://www.plasticsportal.net/wa/plasticsEU~en_GB/portal/show/content/products/biodegradable_plastics/ecoflex_product_literature. Accessed June 18, 2015.

[21] M. A. S. A. Samir, F. Alloin, A. Dufresne, *Biomacromolecules* **2005**, *6*, 612.

[22] X. Z. Zheng, M. G. Forest, R. Vaia, M. Arlen, R. Zhou, *Adv. Mater.* **2007**, *19*, 4039.

[23] H. J. Ploehn, C. Liu, *Ind. Eng. Chem. Res.* **2006**, *45*, 7025.

[24] E. Sabah, S. Ouki, *Int. J. Miner. Process.* **2017**, *162*, 69.

[25] X. Liang, Y. Xu, G. Sun, L. Wang, Y. Sun, Y. Sun, X. Qin, *Chem. Eng. J.* **2011**, *174*, 436.

[26] K. Wojciechowski, G. Z. Zukowska, I. Korczagin, P. Malanowski, *Prog. Org. Coat.* **2015**, *85*, 123.

[27] S. Mukherjee, *The Science of Clay*, Vol. 1, Springer, New Delhi **2013**, p. 54.

[28] M. A. De Paoli, *Degradação e Estabilização de Polímeros*, Vol. 1, Artliber, São Paulo **2009**, p. 247.

[29] B. S. Mitchell, *An Introduction to Materials Engineering and Science for Chemical and Materials Engineers*, John Wiley & Sons, Inc., Hoboken **2004**, p. 901 Appendix 9.

[30] A. Sorrentino, G. Gorrasi, V. Vittoria, in *Environmental Silicate Nano-Biocomposites* (Eds: L. Avérous, E. Pollet), Springer-Verlag, London **2012**, p. 237 Chapter 9.

[31] L. E. J. Nielsen, *Macromol. Sci. Part A Chem.* **1967**, *5*, 929.

[32] H. Adelnia, H. C. Bidsorkhi, A. F. Ismail, T. Matsuura, *Sep. Purif. Technol.* **2015**, *146*, 351.

[33] F. Chivrac, Z. Kadlecová, E. Pollet, L. J. Avérous, *Polym. Environ.* **2006**, *14*, 393.